



Schwinger-Dyson approach to QCD explains the genesis of constituent quark masses^{*}

D. Klabučar^a, D. Kekez^b

^a Physics Department, Faculty of Science, Zagreb University, Bijenička c. 32, 10000 Zagreb, Croatia

^b Rugjer Bošković Institute, Bijenička c. 54, 10000 Zagreb, Croatia

Abstract. Among other successes, the Schwinger-Dyson approach to nonperturbative QCD provides the explanation of the constituent quark model with its quark masses which are very different from the current, Lagrangian masses. Nevertheless, if the interaction kernel contains also the perturbative part of the QCD interaction, the Schwinger-Dyson approach also reproduces the known high-energy behavior of the quark masses predicted by perturbative QCD.

The Schwinger-Dyson (SD) approach to physics of quarks, gluons and hadrons (reviewed, e.g., in Refs. [1–3]) enables the direct contact with their fundamental theory – QCD, through *ab initio* calculations of QCD Green’s functions. Also, SD approach permits many phenomenological applications through various degrees of modeling and approximations, which can nevertheless preserve some crucial features of QCD like its chiral behavior.

In these proceedings we recapitulate from Ref. [4] the part pertaining to the behavior of dressed quark masses, to point out that already several decades ago, the SD approach even at a fairly simple model level provided the correct understanding of the quark masses even in the regime of nonperturbative QCD, and the correct transition between nonperturbative and perturbative regimes of QCD. That is, we explain how SD approach generates dynamically constituent quark masses and thus leads to the constituent quark model in the low energy regime, but is, at the same time, equivalent to the perturbative QCD in the high energy regime if the interaction kernel contains the perturbative QCD part.

Because of nonperturbative features of QCD at low energies, one must consider the strongly dressed two-point quark Green’s function, namely the quark propagator $S(q)$:

$$S^{-1}(q) = A(q^2)\not{q} - B(q^2), \quad (1)$$

is dressed very strongly indeed at low quark energies and momenta q . This means that the propagator “vector function” (i.e., wavefunction renormalization) $A(q^2)$ can noticeably depart from 1, and that (what is much more important qualitatively and quantitatively) the propagator “scalar function” $B(q^2)$ can exceed (at

^{*} Talk delivered by D. Klabučar

low q) the light current masses of the lightest (u and d) quarks drastically, by two orders of magnitude. This is the nonperturbative QCD phenomenon of Dynamical Chiral Symmetry Breaking ($D\chi SB$), which leads to the momentum-dependent quark mass function $\mathcal{M}(q^2) = B(q^2)/A(q^2)$ with values, at low q^2 , of the order of constituent quark masses.

The dressed propagator (1) is obtained by solving the quark two-point (“gap”) SD equation for the appropriate quark flavor. But the big trouble with SD equations is that they are a *coupled system* of integral equations for Green’s functions of QCD, where an equation for a n -point function “calls” not only other n -point functions (and lower), but also $n + 1$ -point functions, leading to the intractable growing tower of SD equations, which must be at some point truncated even in *ab initio* SD calculations. Concretely, the “gap” SD equation for the quark propagator $S(q)$ contains *i*) the dressed gluon propagator $\mathcal{G}_{\mu\nu}(q - k)$ and *ii*) the dressed quark-gluon vertex $\Gamma_\nu(k, q - k, q)$, and they both satisfy their own SD equations. However, such SD calculations in the “*ab initio* research direction” are beyond our present scope. Namely, the crucial insight on the dressed quark masses can anyway be obtained by using an “educated Ansatz” $G_{\mu\nu}(q - k)$ instead of a proper solution $\mathcal{G}_{\mu\nu}(q - k)$ for the the dressed gluon propagator, and by resorting to the commonly used rainbow-ladder approximation (*i.e.*, with bare quark-gluon vertices, $\Gamma_\nu(k, q - k, q) \rightarrow \gamma_\nu$):

$$S^{-1}(q) = \not{q} - \tilde{m} - i g_{st}^2 C_F \int \frac{d^4k}{(2\pi)^4} \gamma^\mu S(k) \gamma^\nu G_{\mu\nu}(q - k), \quad (2)$$

where \tilde{m} is the bare mass term of the pertinent quark flavor, breaking the chiral symmetry explicitly. For the gluon propagator we use one of those which not only lead to $D\chi SB$, but which also provides a remarkably successful description of meson quark-antiquark bound states by the consistent usage in the rainbow-ladder Bethe-Salpeter equation. That is, we use the effective, modeled Landau-gauge gluon propagator of Jain and Munczek [5–7]:

$$g_{st}^2 C_F G^{\mu\nu}(k) = G(-k^2) \left(g^{\mu\nu} - \frac{k^\mu k^\nu}{k^2} \right), \quad (3)$$

where we have indicated that our convention is such that not only the strong coupling constant g_{st} , but also C_F , the second Casimir invariant of the quark representation, are absorbed into the function G . For the present case of $SU(3)_c$, where the group generators are $\lambda^a/2$, namely the (halved) Gell-Mann matrices, $C_F = \frac{4}{3}$.

It is essential that the effective propagator function G is the sum of the perturbative (“ultraviolet”) contribution G_{UV} and the nonperturbative (“infrared”) contribution G_{IR} :

$$G(Q^2) = G_{UV}(Q^2) + G_{IR}(Q^2), \quad (Q^2 = -k^2). \quad (4)$$

The perturbative part G_{UV} is required to reproduce correctly the ultraviolet (UV) asymptotic behavior that unambiguously follows from QCD in its high-energy, perturbative regime. Therefore, this part must essentially be given – up to the factor $1/Q^2$ – by the running coupling constant $\alpha_{st}(Q^2)$ which is well-known from perturbative QCD, so that G_{UV} is in fact *not* modeled.

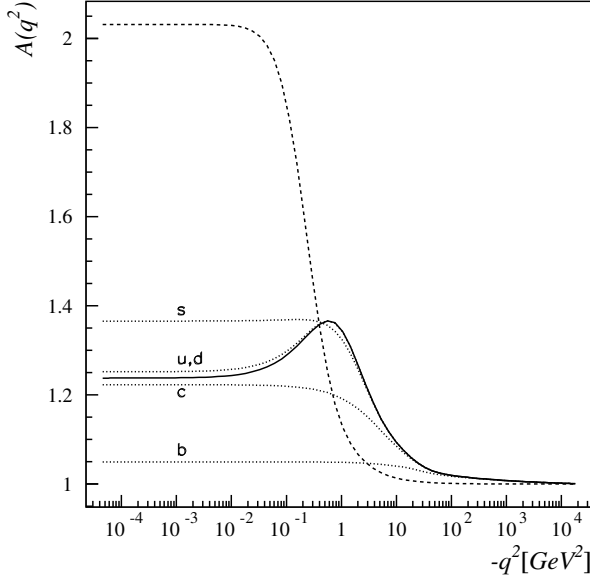


Fig. 1. Our chiral-limit solution (the solid line) for the propagator function $A(q^2)$ is compared with our massive solutions for various $\tilde{m}(\Lambda) \neq 0$ (the dotted lines marked by letters denoting the pertinent flavors). The dashed line denotes the $A(q^2)$ -Ansatz (for u, d-quarks) of [8], and also of Frank *et al.* [9] who have such parameters that the difference with respect to the dashed line [8] cannot be seen on this figure.

From the renormalization group, in the spacelike region ($Q^2 = -k^2$),

$$G_{UV}(Q^2) = 4\pi C_F \frac{\alpha_{st}(Q^2)}{Q^2} \approx \frac{4\pi^2 C_F d}{Q^2 \ln(x_0 + \frac{Q^2}{\Lambda_{QCD}^2})} \left\{ 1 + b \frac{\ln[\ln(x_0 + \frac{Q^2}{\Lambda_{QCD}^2})]}{\ln(x_0 + \frac{Q^2}{\Lambda_{QCD}^2})} \right\}, \quad (5)$$

where we employ the two-loop asymptotic expression for $\alpha_{st}(Q^2)$, and where $d = 12/(33 - 2N_f)$, $b = 2\beta_2/\beta_1^2 = 2(19N_f/12 - 51/4)/(N_f/3 - 11/2)^2$, and N_f is the number of quark flavors. The parameter x_0 is the infrared cutoff, introduced to regulate the logarithmic behavior of G_{UV} as the values of Q^2 approach Λ_{QCD}^2 , the dimensional parameter of QCD. As in [7], we use $x_0 = 10$, but this is not really important since the results are only very weakly sensitive to the values of x_0 , as was already pointed out by [7]. Following [7], we set $N_f = 5$ and $\Lambda_{QCD} = 228 \text{ MeV}$. Although the top quark has meanwhile been found, its mass scale is far above the range of momenta relevant for nonperturbative and bound state calculations, and even above the value of the UV cutoff needed in the massive version of our SD equations (see below). Therefore, there is no need to revise G_{UV} (5) to include $N_f = 6$. (On the other hand, choosing N_f below 5 would not be satisfactory because (i) the momentum range of the order of the b quark mass still has non-negligible influence in our bound-state calculations, (ii) the b quark mass is below the UV cutoff used in our “massive SD equations”, and (iii)

sometimes we need the solutions for relatively high momenta, *e.g.*, to be able to see the asymptotic behavior of the propagator functions $A(q^2)$ and $B(q^2)$ – see Figs. 1, 2 and 3.)

The case $\tilde{m} = 0$ corresponds to the chiral limit where the current quark mass $m = 0$, and where $D\chi SB$ is the one and only cause (“source”) of the constituent quark mass, defined as the mass function value at $q^2 = 0$, namely $\mathcal{M}(0) = B(0)/A(0)$ [5]. Of course, calling “the constituent mass” the value of the “momentum-dependent constituent mass function” $B(q^2)/A(q^2)$ at exactly $q^2 = 0$ and not on some other low q^2 , is a matter of a somewhat arbitrary choice. Another conventional choice (*e.g.*, in [10]) is to call the solution of $-q^2 = B^2(q^2)/A^2(q^2)$ the Euclidean constituent-quark mass squared. However, since this is just a matter of choosing terminology, we stick to that of Jain and Munczek [6].

With the assumption that u and d quarks are massless, which is an excellent approximation in the context of hadronic physics, solving of (2) yields the solutions for $A(q^2)$ and $B(q^2)$, displayed in respective Fig. 1 and Fig. 2 by the solid lines.

In these figures we also compare them with $A(q^2)$ and $B(q^2)$ corresponding to the dressed propagator *Ansätze* of the references [8,9], represented by the dashed lines. Our massless solutions lead to the constituent u (and d) quark mass $B(0)/A(0) = 356$ MeV. The ratio $B(q^2)/A(q^2)$, namely our momentum-dependent mass function $\mathcal{M}(q^2)$, is depicted in Fig. 3 by the solid line, and the dashed line represents the analogous ratio formed from $A(q^2)$ and $B(q^2)$ corresponding to the *Ansätze* of Refs. [8,9].

Note that our chiral-limit solutions for $A(q^2)$ and $B(q^2)$ differ a lot from the *Ansätze* of Refs. [8,9], even though the ratio, giving the mass function, is similar.

When $\tilde{m} \neq 0$, the SD equation (2) must be regularized by a UV cutoff Λ [6,7], and the bare mass \tilde{m} is in fact a cutoff-dependent quantity. We adopted the parameters of [7], where (for $\Lambda = 134$ GeV) $\tilde{m}(\Lambda^2)$ is 3.1 MeV for the isosymmetric u- and d-quarks, 73 MeV for s-quarks, 680 MeV for c-quarks, and 3.3 GeV for b-quarks. Solving of (2) then yields the solutions $A(q^2)$ and $B(q^2)$ for “slightly massive” u- and d-quarks, “intermediately massive” s-quarks, as well as the solutions for the heavy quarks c and b. We essentially reproduce the results of Ref. [7] (within the accuracy permitted by numerical uncertainties). The $A(q^2)$ and $B(q^2)$ solutions for $\tilde{m}(\Lambda^2) \neq 0$ are displayed in Figs. 1 and 2 by dotted lines marked by u, d and s, c and b, indicating which flavor a curve pertains to. For the lightest, u- and d-quarks (with $\tilde{m} = 3.1$ MeV), both $A(q^2)$ and $B(q^2)$ are only slightly above the curves representing our respective chiral-limit solutions. More precisely, the difference is then at most 1.4% (at $q^2 = 0$) for $A(q^2)$, while for $B(q^2)$ the largest absolute value of the difference (again occurring at $q^2 = 0$) amounts to an excess of 6.2% over our chiral-limit solution. The excess quickly becomes much smaller above $-q^2 = 0.2$ GeV. Admittedly, at $-q^2$ above 2 GeV, the *relative* difference between the “chiral” and “slightly massive” $B(q^2)$ ’s starts growing again because of the different asymptotic behaviors of these respective solutions. They are, respectively, $B(q^2) \sim [\ln(-q^2/\Lambda_{QCD}^2)]^{d-1}/q^2$ and $B(q^2) \sim 1/[\ln(-q^2/\Lambda_{QCD}^2)]^d$, and are consistent with the asymptotic freedom of QCD [11, 12]. (This in turn results in the asymptotic behavior of the momentum-

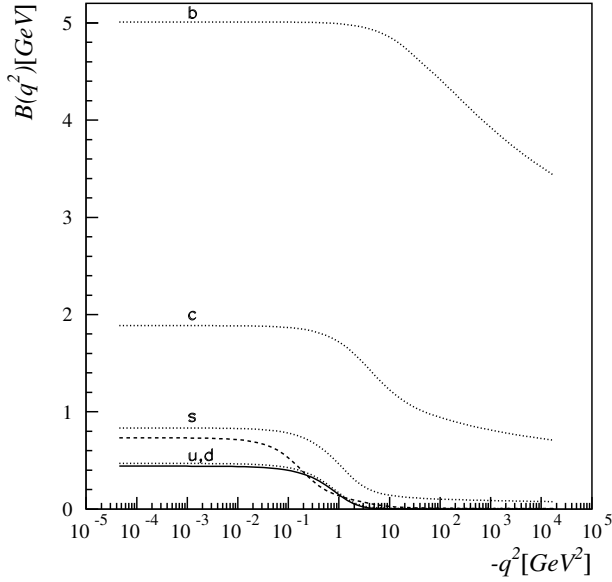


Fig. 2. The comparison of our chiral-limit solution (the solid line) for the propagator function $B(q^2)$ with our massive solutions for various $\tilde{m}(\Lambda) \neq 0$ represented by the dotted lines marked by letters denoting the pertinent flavors, and with the *Ansatz* (for u, d-quarks) for $B(q^2)$ employed by [8] (the dashed line), and that of [9], which cannot be distinguished from the dashed line in this plot.

dependent, dynamical mass functions $B(q^2)/A(q^2)$, which is in accord with the behavior in perturbative QCD [5–7,12,13]). However, the absolute values of these $B(q^2)$'s (even for the “slightly massive” case) and of their difference are already very small at $-q^2 > 2$ GeV.

The deep Euclidean asymptotic behavior $B(q^2) \sim 1/[\ln(-q^2/\Lambda_{\text{QCD}}^2)]^d$ is fulfilled also for the more massive flavors, but of course with very different coefficients (which are essentially proportional to the current quark masses [6,7]). Also, $A(q^2) \rightarrow 1$ for all flavors as $-q^2 \rightarrow \infty$. For low $-q^2$, however, $A(q^2)$'s belonging to different flavors exhibit interesting differences. The bump that characterizes the least massive (or chiral) u, d-quarks is absent already in $A(q^2)$ of our “intermediately massive” s-quark, for which the fall-off is almost monotonical, as the increase (around $-q^2 \sim 0.1$ GeV) above the $A(0)$ -value is practically imperceptibly small. Moreover, for even heavier c– and especially b–quarks, the $A(q^2)$ -values for even lowest $-q^2$'s, are below the corresponding values of the chiral-limit $A(q^2)$. Comparing the various $A(q^2)$ - and $B(q^2)$ -solutions illustrates well how the importance of the dynamical dressing decreases as one considers increasingly massive quark flavors.

These $\tilde{m} \neq 0$ solutions give us the constituent mass $B(0)/A(0)$ of 375 MeV for the (isosymmetric) u- and d-quarks, 610 MeV for the s-quarks, 1.54 GeV for the c-quarks, and 4.77 GeV for the b-quarks. These are very reasonable values. Also,

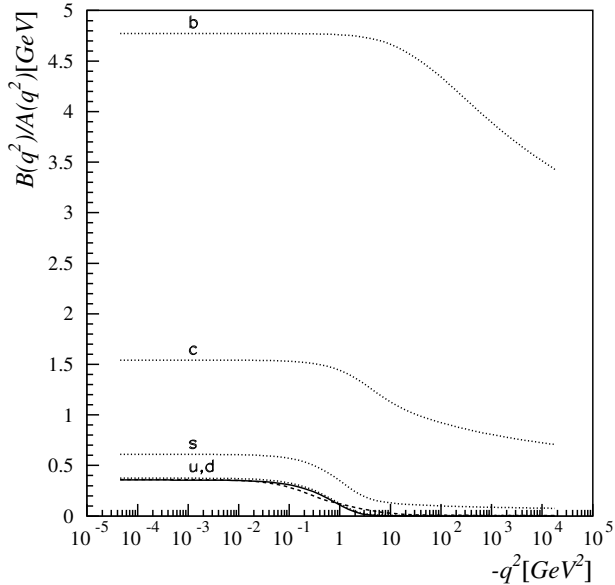


Fig. 3. The solid line denotes our constituent quark mass function $B(q^2)/A(q^2)$ in the chiral limit, while the dotted lines (marked by letters indicating the pertinent flavors) denote our constituent quark mass functions for $\tilde{m}(\Lambda) \neq 0$. The one following from the *Ansätze* of [8,9] is denoted by the dashed line.

the momentum-dependent mass functions $B(q^2)/A(q^2)$ – depicted in Fig. 3 – in the presently chosen variant of the SD approach [5–7] behave for all flavors in the way which correctly captures the differences between heavy and light quarks and qualitatively agrees with the most advanced recent results on the quark masses in the SD approach such as Ref. [14], where instead of simple regularization [6,7] the full nonperturbative renormalization has been carried out and the quantitative agreement with quenched lattice results achieved over a very wide range of momenta.

Acknowledgments. This work has been supported in part by the Croatian Science Foundation under the project number 8799. The authors acknowledge the partial support of the COST Action MP1304 “Exploring fundamental physics with compact stars (NewCompStar)”.

References

1. C. D. Roberts and A. G. Williams, *Prog. Part. Nucl. Phys.* **33**, 477 (1994).
2. R. Alkofer and L. von Smekal, *Phys. Rept.* **353**, 281 (2001) [hep-ph/0007355].
3. I. C. Cloet and C. D. Roberts, *Prog. Part. Nucl. Phys.* **77**, 1 (2014) [arXiv:1310.2651 [nucl-th]].
4. D. Kekez, B. Bistrovic and D. Klabucar, *Int. J. Mod. Phys. A* **14**, 161 (1999) [hep-ph/9809245].

5. P. Jain and H. J. Munczek, *Phys. Rev.* **D44**, 1873 (1991).
6. H. J. Munczek and P. Jain, *Phys. Rev.* **D46**, 438 (1992).
7. P. Jain and H. J. Munczek, *Phys. Rev.* **D48**, 5403 (1993).
8. C. D. Roberts, *Nucl. Phys.* **A605**, 475 (1996)
C. D. Roberts, in: *Chiral Dynamics: Theory and Experiment*, eds. A. M. Bernstein and B. R. Holstein, *Lecture Notes in Physics*, Vol. **452** (Springer, Berlin, 1995) p. 68.
9. M. R. Frank, K. L. Mitchell, C. D. Roberts and P. C. Tandy, *Phys. Lett.* **B359**, 17 (1995).
10. P. Maris and C. D. Roberts, *Phys. Rev.* **C56**, 3369 (1997).
11. K. Lane, *Phys. Rev.* **D10**, 2605 (1974).
12. H. D. Politzer, *Nucl. Phys.* **B117**, 397 (1976).
13. R. Tarrach, *Nucl. Phys.* **B183**, 384 (1981).
14. M. S. Bhagwat, M. A. Pichowsky, C. D. Roberts and P. C. Tandy, *Phys. Rev. C* **68**, 015203 (2003) [nucl-th/0304003].

Kvarkovska snov v močnih magnetnih poljih

Débora Peres Menezes

Universidade Federal de Santa Catarina, Departamento de Física-CFM-CP 476, Campus Universitário-Trindade, CEP 88040-900, Florianópolis-SC, Brazil

V pričujočem prispevku skušamo razumeti razne lastnosti kvarkovske snovi, kot jih opisuje model Nambuja in Jona-Lasinia v prisotnosti močnih magnetnih polj. Najprej analiziramo raznovrstne fazne diagrame. Potem raziskujemo razlike, ki nastanejo zaradi različnih vektorskih interakcij v Lagrangeovi gostoti in uporabimo izsledke za opis zvezdne snovi. Nato se ozremo na značilnosti dekonfinacije in vzpostavitev kiralne simetrije pri kemičnem potencialu nič v okviru prepletene Polyakovove verzije modela Nambuja in Jona-Lasinia. Končno proučimo lego kritične točke za različne izbire kemičnega potenciala in gostote.

Schwinger-Dysonov pristop h kvantni kromodinamiki razloži nastanek oblečenih mas kvarkov

D. Klabučar^a in D. Kekez^b

^a Physics Department, Faculty of Science, Zagreb University, Bijenička c. 32, 10000 Zagreb, Croatia

^b Rugjer Bošković Institute, Bijenička c. 54, 10000 Zagreb, Croatia

Poleg drugih uspehov Schwinger-Dysonov pristop k neperturbativni kvantni kromodinamiki razloži tudi to, zakaj so v efektivnih kvarkovih modelih oblečene mase kvarkov zelo različne od golih mas. Če pa interakcijsko jedro vsebuje tudi perturbativni delež kromodinamske interakcije, poda Schwinger-Dysonov pristop tudi znano visokoenergijsko obnašanje kvarkovih mas, tako kot jih napoveduje perturbativna kvantna kromodinamika.

Mezonski učinki pri osnovnih in resonančnih stanjih barionov

R. Kleinhappel^a, L. Canton^b, W. Plessas^a in W. Schweiger^a

^a Theoretical Physics, Institute of Physics, University of Graz, Universitätsplatz 5, A-8010 Graz, Austria

^b Istituto Nazionale di Fisica Nucleare, Via F. Marzolo 8, I-35131 Padova, Italy

Za raziskavo mezonskih učinkov pri osnovnih in resonančnih stanjih barionov smo vključili mezonske zanke v relativistični pristop s sklopljenimi kanali. Iz računov, ki so bili doslej napravljeni na hadronskem nivoju, smo dobili rezultate za oblečene mase osnovnega stanja in resonanc nukleona. S sklopitvijo na pionski kanal smo dobili tudi širine resonanc, zlasti resonance Δ . Za zdaj smo sicer izboljšali rezultate v primerjavi z računi z enim samim kanalom, vendar so razpadne širine še vedno premajhne v primerjavi z meritvami.